Eur Respir J, 1994, 7, 2038–2045
DOI: 10.1183/09031936.94.07112038
Printed in UK - all rights reserved

European Respiratory Journal
ISSN 0903 - 1936

Theoretical and experimental basis for the development of a dynamic airway stent

L. Freitag, R. Eicker, B. Linz, D. Greschuchna

Theoretical and experimental basis for the development of a dynamic airway stent. L. Freitag, R. Eicker, B. Linz, D. Greschuchna. ©ERS Journals Ltd 1994.

ABSTRACT: Three major problems are currently associated with airway stents: mucostasis, formation of granulation tissue, and migration. We wanted to determine whether these problems could be solved by a different stent design.

Based on theoretical considerations of an idealized trachea, we developed a dynamic bifurcation stent made of silicone which incorporates horseshoe-shaped steel struts. A flexible posterior membrane enables dynamic compression during cough, whilst the clasps maintain the airway lumen in the face of external compression. The design of the stent cast was based upon computed tomographic (CT)-scan studies of the central airways. Its complex shape provides a smoother distribution of pressure on the mucosa; thereby, lowering the stimulus for granulation formation. The bronchial limbs saddle on the carina, preventing displacement.

The mechanical behaviours of the new stent and two commercially available stents were compared in an *ex-vivo* model, utilizing freshly excised tracheae and new visualization techniques. Dynamic (artificial coughs) and static loads (simulating tumour compression or pleural pressures) were applied on excised human tracheae with different stents. Our dynamic stent preserved effective compression of the posterior membrane in response to cough, and also provided lumen stability against extrinsic compression. In comparison, the two commercially available stents did not provide both functions equally well.

In conclusion, our newly designed dynamic bifurcation stent shows characteristics which should prove useful in avoiding problems currently associated with airway stents.

Eur Respir J., 1994, 7, 2038–2045.

Ruhrlandklinik, Center for Pulmonary Medicine and Thoracic Surgery, Essen, Germany.

Correspondence: L. Freitag
c\o Ruhrlandklinik
Centre for Pulmonary Medicine and Thoracic Surgery
45239 Essen
Germany

Keywords: Bifurcated airway stent
bronchial cancer
dynamic stent
mucus clearance
tracheal stenosis

Received: March 14 1994
Accepted after revision July 30 1994

The bronchoscopic placement of endoprostheses into obstructed airways has become an increasingly accepted therapeutic approach. Over the last 5 yrs, we have inserted nearly 400 stents into patients suffering from benign or malignant stenoses, tracheomalacia or fistulae. A variety of metal and silicone prostheses is available [1–8]. In most cases of central airway stenosis silastic stents have been used, whilst segmental bronchi stenoses have mainly been treated with various metal stents [9].

The following problems were frequently encountered 1) accumulation of inspissated secretions inside the prostheses; 2) development of granulation tissue at the edges of stents, with overgrowth of the airway lumen; and 3) migration of the stents.

In our experience, approximately 15% of all patients with silastic stents or T-tubes develop clinically significant obstruction of the stent with inspissated secretions (fig. 1). This phenomenon can be observed regardless of the stent material or its surface coating. One reason for this is the fact that there is no ciliary clearance inside the silicone stents. Moreover, stents do not permit effective cough, an important mechanism for clearance of excessive secretions even in the absence of ciliary beating [10].

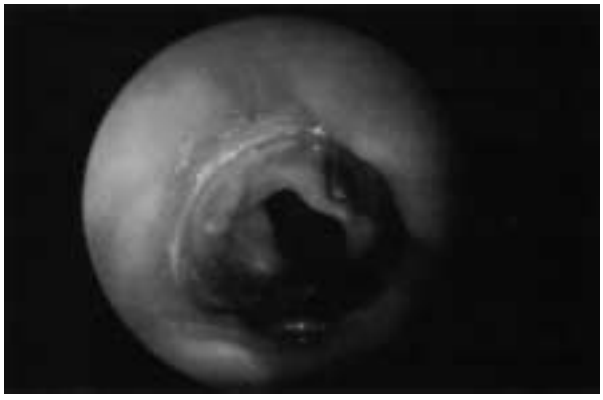

Fig. 1. – Inspissated secretion inside a silicone stent. Mucosa above and below prosthesis is normal.

Normally, the airways, including the trachea, are dynamic. The critical velocity of airflow necessary to move mucus is achieved, in part, by dynamic reduction of cross-sectional area [11–13]. Most commercially available stents are stiff, and do not respond sufficiently to changes of transmural pressure during forced exhalation or coughing. Therefore, in a stented airway, adequate

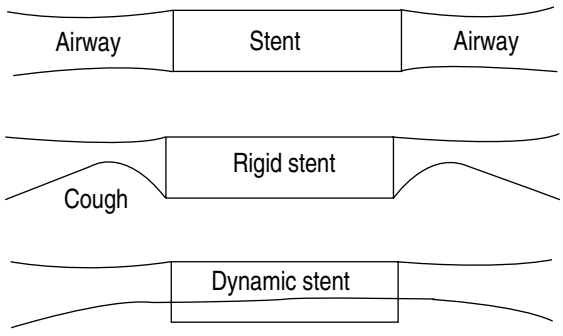

Fig. 2. – Diagrammatic representation of change in diameter of normal trachea, trachea with rigid stent during cough, and trachea with dynamic stent during cough. As flow is equal along the airway, velocity and, thereby, interfacial shear stress is lowest inside the rigid stent.

velocities and shear-forces can hardly be established. Thus, a basic feature of a stent for long-term use should be the ability to respond to cough pressures with reversible reduction of cross-sectional area (fig. 2). In order to accomplish this, the stent was designed with a flexible posterior membrane.

Granulation tissue frequently develops at the edges of endotracheal tubes and stents. In agreement with the literature [14], we have observed a higher incidence of excessive granuloma formation with metal stents. It is possible that the metal itself might be the crucial stimulus [15]. On the other hand, scars and granulation stenoses are more likely to develop if high localized pressures (*e.g.* from a tube cuff) on the mucosa reduce capillary perfusion and impair tissue nutrition [16, 17]. Thus, the high rate of granuloma formation, especially with spring-loaded Gianturco stents, might be ascribed to the disadvantageous relationship between small contact area (with high locally applied pressure from the thin coils of the spring) to the much larger tissue surface involved. In order to distribute the pressure as equally as possible over the mucosal surface, we tried to match, as closely as possible, the shape of the stent with the shape of the trachea and first generation bronchi.

The outer surface of Dumon silicone stents bears regularly placed pitted studs to ensure adherence to the airway wall [6]. ORLOWSKI [3] stents have circular silicone rings to avoid intratracheal migration. However, in spite of these innovations, migration frequently occurs with silastic stents. In the trachea, in particular, displacements can be observed in up to 20% if the stenosis fails to support a stent, a problem often encountered in tracheal fistulae. Transcutaneous fixation with threads has been suggested, but due to the high incidence of inflammatory complications, including fistula formation, we have abandoned this technique. The barbs of Gianturco stents [4, 5] help to prevent migration but they make later repositioning or removal difficult. Thus, we designed a bifurcating stent saddling on the main carina. The bifurcation inhibits the stent from twisting or migrating, but allows for easy bronchoscopic removal.

Based upon theoretical considerations, laboratory experiments in excised tracheae lead to the development of a new airway stent addressing these three problems.

Material and methods

The experimental work consisted of two parts, shape design and tests of biomechanical behaviour. For the shape design of a dynamic stent, radiological measurements of the central airways were made. The data acquired were used to produce casts for stents. A test series of stents from these casts was made and studies of mechanical behaviour were performed, utilizing an *ex-vivo* human trachea model. Biomechanical experiments included cough studies, stress-strain measurements under different pleural pressures, and studies of behaviour under simulated tumour compression.

Shape design of the dynamic stent

In order to match the shape of the stent to the human airways, computed tomography (CT) was used as an elegant tool to obtain information about the internal contour of the trachea and bronchi, *in situ* [18, 19]. To cast an airway stent, a detailed blueprint was necessary. One hundred and fifty randomly selected CT scans of adult patients were analysed. The patients suffered from various lung diseases, not involving the trachea. The scans were enlarged by a factor of five and placed on a digitizer (Genitizer 1212). Polar co-ordinates (36 points·scan^{-1}) of the tracheal edges were fed into a microcomputer. The data were processed with a statistic program (Systat 5.0) and average shapes at three levels (1 cm below the vocal cords, middle of trachea and 1 cm above the carina) were calculated. From the reconstructed pictures, bifurcation angles between trachea and main bronchi were obtained. These data were processed with a computer-aided design (CAD) program (Design CAD 3D, American Small Business Co.). From the CAD data, casts for bifurcation stents of three sizes (see Results) were manufactured (Rüsch AG, Kernen, Germany).

Stress-strain measurements in excised trachea

Stress-strain measurements of human tracheae with different stents were carried out in a test chamber. The set-up (fig. 3) permitted studies of biomechanical behaviour under conditions of forced expiration, cough, and extrinsic compression, modelling the effect of tumours or inflammatory processes.

The tracheae were placed into a Plexiglas chamber with a glass window at one side. Through this window, inward bulging and other deformations of the trachea or of stents placed inside tracheae could be observed under different conditions. Using a vacuum or a pressure source with a water seal connected to the chamber, negative or positive transmural static pressures could be applied. Rapid pressure changes emulating cough were applied, "intraluminal" and "pleural", by a cough generator. The cough generator consisted of a diaphragm driven by a computer-controlled vibration testing device. Transtracheal pressure swings of +5 to -9 kPa could be generated,

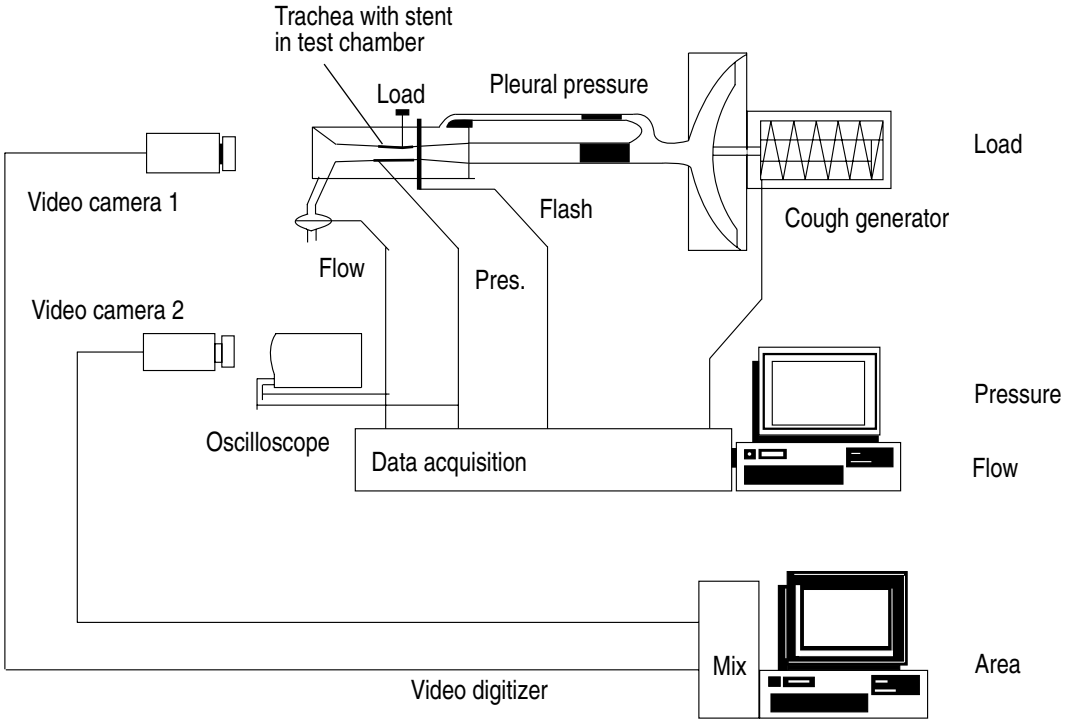

Fig. 3. – Experimental set-up for testing of static and dynamic behaviour of tracheae with stents. Artificial coughs, pleural pressures and tumour compression from any side can be simulated.

reaching flows up to 9 $l \cdot s^{-1}$. The cough generator has been described in detail previously [20]. The distal ends of the tracheae were attached to a 10 *l* tank acting as a lung surrogate.

Loads, simulating tumour compression could be applied to the outside of the excised tracheae with a small rounded aluminum rod of 3 mm diameter. A ring flash around the Plexiglas chamber served to illuminate the area-section of interest. A video-camera with a macro lens was mounted in front of the glass window. Triggering the flash on changes in pleural pressures or on the phase of the cough generator permitted sequential analyses of forced expiration and coughing manoeuvres.

Video images were digitized and the cross-sectional areas of the tracheae were calculated on an Amiga 2000 computer (Commodore), using an inhouse written planimetry program. Transmural pressures, loads, and cough flows were measured with standard instruments, fed into a microcomputer and displayed on a storage oscilloscope. Area-pressure curves and area-load curves were plotted using a spreadsheet program on a PC.

In order to simulate extrinsic compression of the trachea by a tumour or inflammatory process, a variable load was placed on the trachea either laterally or on the posterior membranous portion. The stress-strain measurements were performed in excised tracheae alone, and repeated in tracheae with various airway stents. The measurements with stents in place were made in random order with a Dumon silastic stent, cut to 25 mm length (Endoxane 16/30, Cometh, Marseille, France) and a 25 mm long piece of the Dynamic stent (prototype supplied by Rüsch, Kernen, Germany), followed by measurements with a Gianturco stainless steel Z-stent (type 15/25 William Cook Co. Europe, Bjaeverskov, Denmark). Removal of the Gianturco stent was difficult without damaging the surface of the trachea, necessitating the use of this stent at the end of the series of measurements.

Results

Shape design

The average sizes and shapes obtained at three levels of the tracheae are shown in figure 4. The branching angles between trachea and the main bronchi were measured as 144.7±4° to the right and 133.3±3° to the left. Below the cricoid, the average trachea had a longitudinally oval shape, emerging *via* a round-shaped middle section towards a transversely oval shape near the bifurcation. Figure 5 shows the dynamic bifurcated stent. Three sizes of stents were manufactured, representing the mean size±1 SD. The shapes of the three sections, as shown on the left side of the picture, are derived from the CT data in figure 4.

Stress-strain measurements

The cross-sectional area of the lumen of excised tracheae were measured under conditions simulating a cough by applying rapid transtracheal pressure swings of +3 to -9 kPa with a $\Delta P/\Delta t$ slope of 90 $kPa \cdot s^{-1}$ with

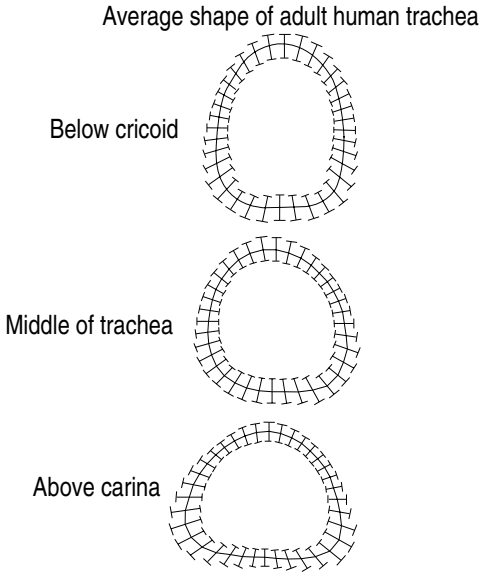

Fig. 4. – Mean shape of trachea at three levels derived from 150 compu-ted tomographic (CT)-scans. Lower and higher standard deviation of the mean are indicated by the bars.

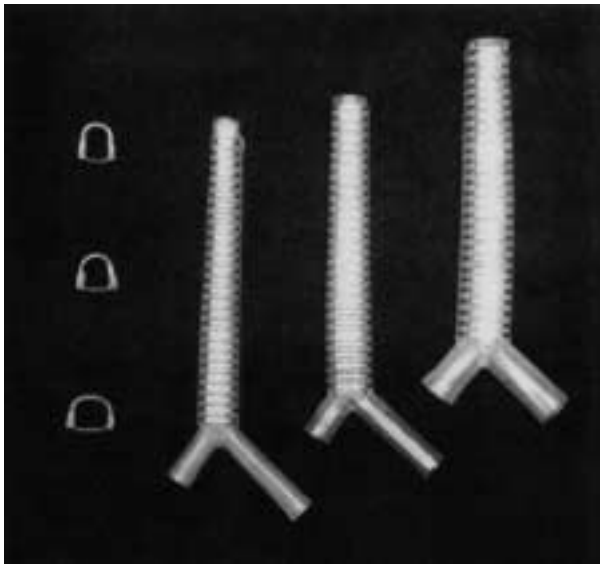

Fig. 5. – Three sizes of dynamic Y-stents representing mean, lower and higher standard deviation of the mean of data from figure 4. Stent can be cut to desired length.

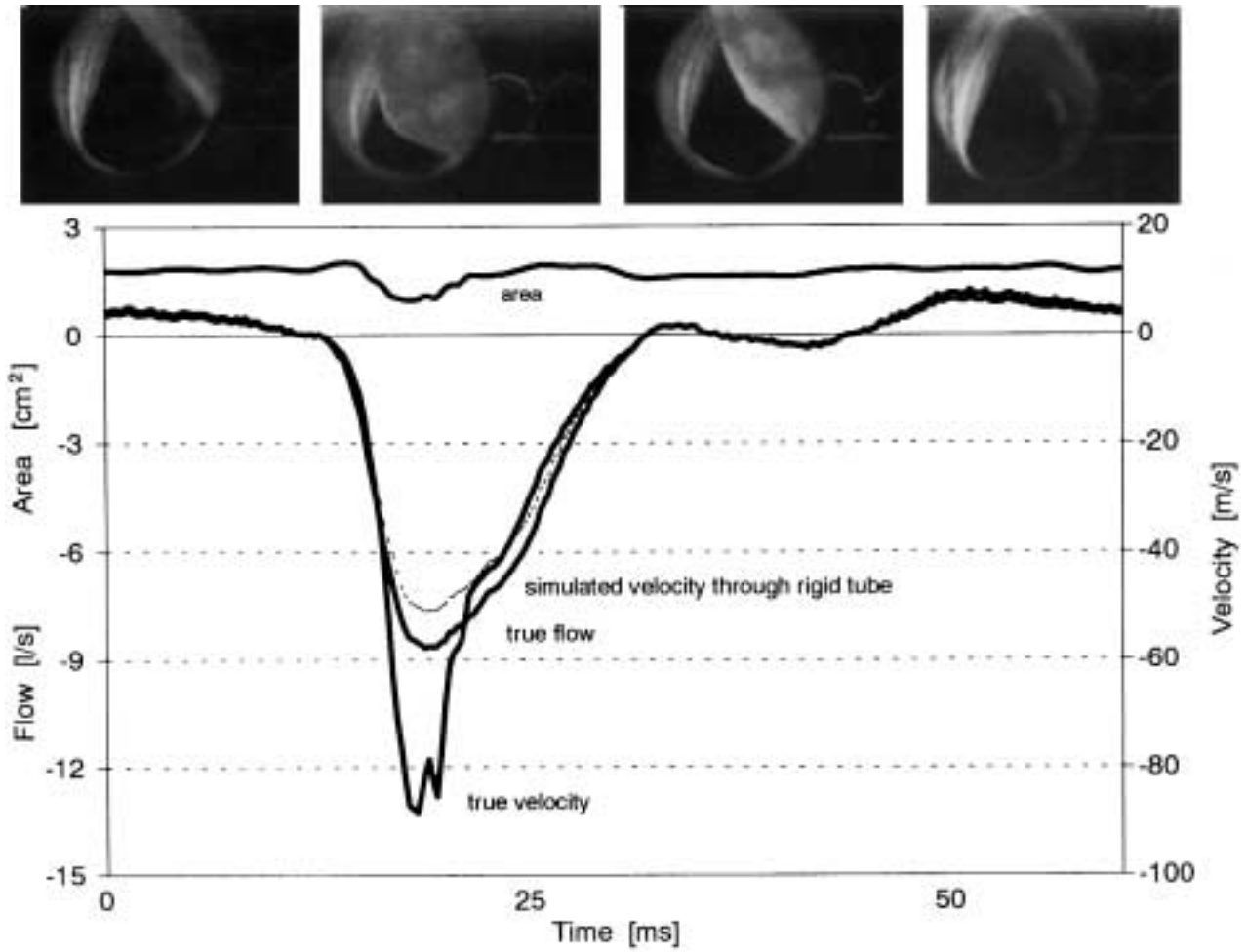

Fig. 6. – Artificial cough in excised human trachea. High gas velocity (flow/area) is accomplished by partial airway collapse at time of peak flow. Inward bulging of posterior membrane is essential to achieve sufficient interfacial shear stress on mucous layer.

the cough generator. Figure 6 shows a typical velocity curve.

As the peak expiratory flow of 8.1 $l \cdot s^{-1}$ matches the minimum of cross-sectional area, the true peak flow velocity reaches 87 $m \cdot s^{-1}$. For comparison, figure 6 includes a plot for a rigid trachea with a cross-sectional area of 1.8 cm^2. It demonstrates that for a rigid trachea (or for a rigid stent) peak flow velocity would not exceed 50 $m \cdot s^{-1}$.

Static compliance curves of seven tracheae were obtained by applying transmural pressures, which were increased in steps of 0.1 kPa from 0 to 20 kPa. The compliance curves showed variations depending on the shape of the trachea and the age and medical condition of the patient at death. Although the absolute values of the slopes differed, their geometrical shapes were similar.

Stents were placed inside the tracheae and the runs were repeated. The results, relevant for the development of the dynamic stent, are shown for one representative trachea. Area-pressure and area-load relationships of this trachea with three different types of stents (same diameter) are displayed in figures 7–9.

The compliance curve (area *vs* pleural pressure) (fig. 7) of an isolated trachea has an exponential shape. With a Dumon silastic stent the area-pressure curve of the trachea is more linear. While the area is approximately 10% of a_0 at 10 kPa in the trachea alone, it increases to approximately 50% of a_0 with the Dumon stent. The Gianturco stent does not change the compliance curve decisively. With a dynamic stent, the compliance curve remains exponential but has an offset. At 10 kPa the actual cross-sectional area increases to 18%, compared to 10% for the trachea without stent.

The area *vs* load from side curve of the trachea (fig. 8) is linearly shaped. This shape remains while the slope is heavily affected by the stent placement. The Dumon silastic stent and the dynamic stent add significant stability, while the additional recoil effect of the Gianturco is lower than the resolution of the measuring apparatus.

Loaded from the posterior membrane (fig. 9) both the Dumon stent and the dynamic stent help to retain a sufficient lumen, whilst the Gianturco stent adds only little to the recoil of the isolated trachea.

Figure 10 shows compliance curves of two tracheae, alone and with a dynamic stent (silicone hardness 60 Shore). The compliance curves of the trachea from a patient who had emphysema is significantly steeper than the curve of the trachea from the patient who died of heart failure without history of pulmonary disease. However, the curves after stent placement show hardly any difference, demonstrating that compared to the stiffness of the stent, variations of the compliance of normal tracheae are negligible.

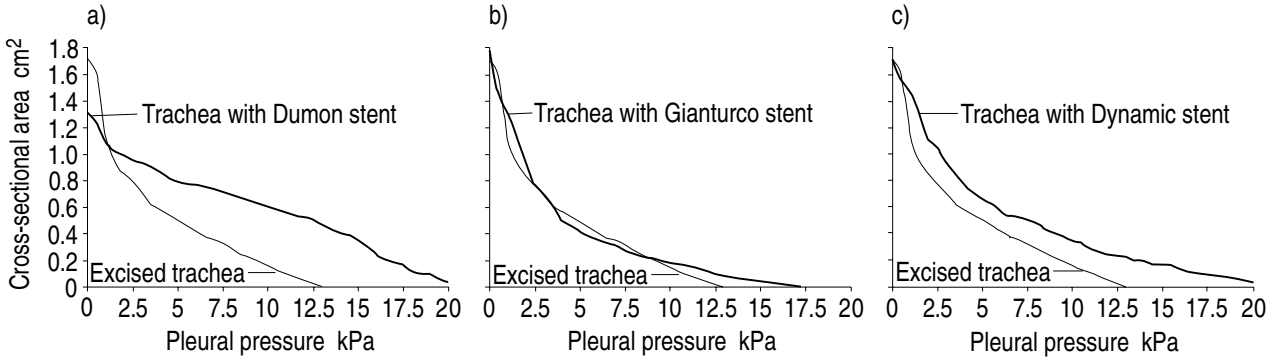

Fig. 7. – Mechanical behaviour (area *vs* pleural pressure) of isolated human trachea with three different stents of comparable diameter. a) Trachea and trachea with Dumon silicone stent. b) Trachea and trachea with self-expanding Gianturco steel stent. c) Trachea and trachea with dynamic stent.

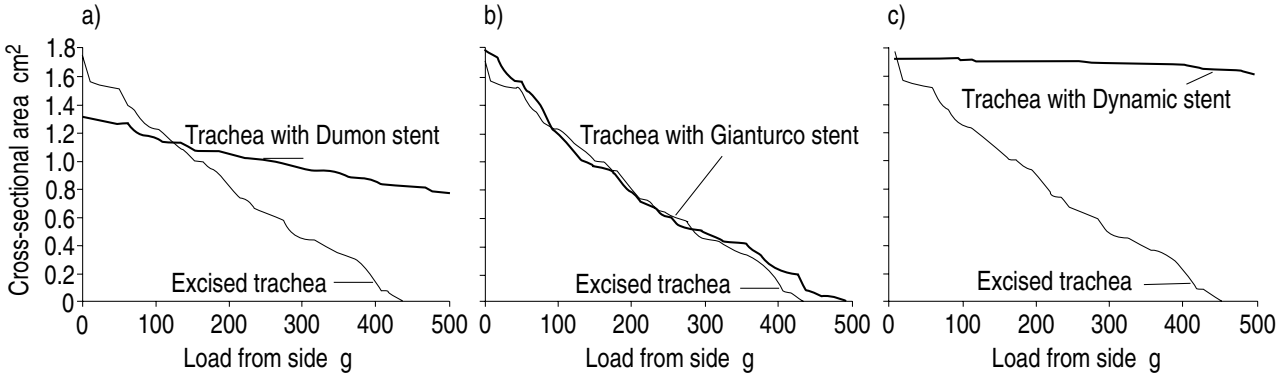

Fig. 8. – Mechanical behaviour (area *vs* load from side) of isolated human trachea with different stents under simulated lateral tumour compression. a) Trachea and trachea with Dumon silicone stent. b) Trachea and trachea with self-expanding Gianturco steel stent. c) Trachea and trachea with dynamic stent.

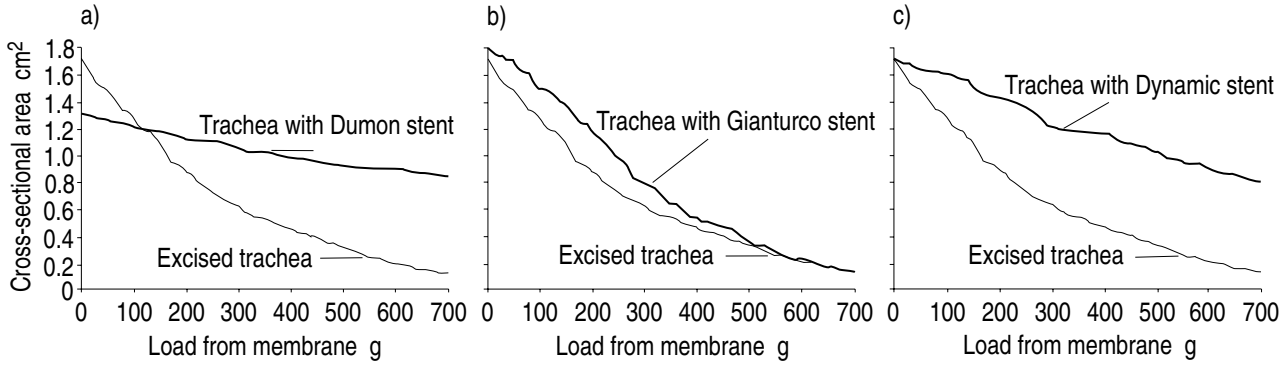

Fig. 9. – Mechanical behaviour (area *vs* load from posterior membrane) of isolated human trachea with different stents under simulated tumour compression. a) Trachea and trachea with Dumon silicone stent. b) Trachea and trachea with self-expanding Gianturco steel stent. c) Trachea and trachea with dynamic stent.

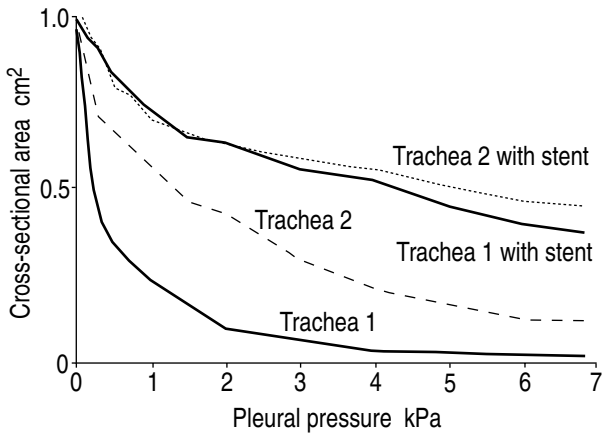

Fig. 10. – Mechanical behaviour of two tracheae with opposite characteristics, alone and with dynamic stents. Trachea 1 is from an emphysema patient, trachea 2 (dotted) from a patient without history of pulmonary disease.

Discussion

Theoretical considerations have led to the design of an airway stent which minimizes stent associated problems.

Self-expanding wire stents, such as the Gianturco Z-stent or balloon-expanded Palmaz stents, are eventually covered by epithelium. Thus, ciliary mucus clearance can be re-established to a limited extent [21]. However, their use is limited by some considerations, including: possible tumour growth through the wire meshes, danger of perforation, and irreversibility of placement. Due to their low recoil force, these metal stents cannot resist marked tumour compression. They are not feasible to seal tracheo-oesophageal fistulae. Thus, for most palliative procedures, silicone stents, silicone-coated metal stents, or combinations of metal and rubber stents have proved to be superior. However, using an indwelling silicone rubber stent excludes any ciliary-dependent clearance, and retained secretions can become a clinically relevant problem. Without ciliary clearance, sputum must be expelled by cough or, less efficiently, by respirations.

Any airstream flowing through a tube with liquid-covered walls creates an interfacial shear force on that liquid layer. Above a certain threshold (depending on thickness and rheology of the liquid and the velocity and density of the gas) the fluid starts to move in the same direction as the gas stream. For annular flow through a wet tube the interfacial shear stress can be calculated as:

$$\tau_i = \frac{1}{2} C_{f,i} \cdot \rho_a \cdot U^2$$

where τ_i is the interfacial shear stress, $C_{f,i}$ is the interfacial friction factor, ρ_a is the density of air, and U is the mean velocity of airflow [21].

It has been shown [22, 23] that this equation is applicable to the gas/liquid interaction in the airways of patients with bronchial hypersecretion. It follows that the shear force on the mucous layer covering the tracheobronchial walls is proportional to the velocity of airflow to the power of two. The velocity ($cm \cdot s^{-1}$) is flow ($cm^3 \cdot s^{-1}$) divided by cross-sectional area (cm^2) and, thus, the shear force is inversely related to the square of the cross-sectional area. Figure 6 shows flow, area and velocity curves in a representative trachea in the test chamber during an artificial cough. The reduction of cross-sectional area by dynamic compression during maximum flow contributed substantially to the achievement of high flow velocity [24]. The calculated velocity curve for a completely rigid trachea underscores the importance of this effect.

In vivo studies of subjects with chronic bronchitis have shown maximum reduction in tracheal diameter during coughing of 33.7±4.8% in the trachea and 28.6± 7.1% in the main bronchi [13]. In patients with flow limitation due to chronic bronchitis or tumour obstruction, dynamic area reduction becomes an essential factor for effective cough clearance.

Airway stents, however, by their very nature have to be stiff. Intended to counterbalance tumour pressures, they oppose the desirable dynamic area reduction during coughs. Under circumferential (pleural) pressure, simple silastic tubes show a nearly linear pressure-area relationship, rather different from the behaviour of real airways. For Gianturco stents a hyperbolic function for wall-extending force *versus* radial displacement was found empirically [25]. The unique pressure-area

behaviour of a trachea can be expressed mathematically with the classic Shapiro equation [26, 27].

$$A=A_0 (1 - P/P_1)^{-n}$$

Where n, ranging between 0.5 and 1, varies depending mainly on the compliance of the tissue and deformation features of the cartilages [28]. The reduction of cross-sectional area is caused mainly by invagination of the posterior membrane and only in part by deformation of the cartilages [29].

The tested Gianturco stent shows ideal coughing behaviour. However, it can resist hardly any tumour compression exceeding the extensible forces of the real trachea. Z-stents with different wires or diameters might be more feasible for tumour treatment, but we tested the one that is commercially available and recommended by the manufacturer. The cylindrical Dumon silicone stent can alleviate a considerable load, but has a more linear area-pressure behaviour during cough.

The curves show that the desired opposing requirements are fulfilled best by the combined steel-silicone construction. The dynamic stent can counterbalance loads of up to 600 g on the side and even on the membranous part without significant reduction in cross-sectional area. Under cough conditions, the pressure-area behaviour is geometrically nearly identical to the behaviour of the trachea alone, but with an additional offset. The offset depends on the elasticity of the steel and the hardness of the silicone. We found the combination shown here suitable for most clinical problems. The invagination of the posterior membrane with a reduction of cross-sectional area of 25% under cough is comparable to the behaviour of the normal trachea.

As the total stiffness in the stented airway is the sum of the intrinsic stability of the trachea and the recoil of the stent, it might be necessary to develop stents with various hardnesses for different diseases. Malacia or a tracheo-oesophageal fistula might be better treated with a more compliant model; whereas, lymph-node compression might require a stiffer stent. By changing the number of steel struts in the dynamic stent or the hardness of its silicone, these aims can easily be achieved. It could also be useful to replace the steel struts with temperature dependent Nitinol shape memory alloy. After folding it together in cold liquid, insertion of the prosthesis would be facilitated. At body temperature, the dynamic stent would expand, regaining its biomechanical advantages.

Impaired mucosal blood supply is a key factor for the development of granulation tissue. In order to minimize the pressure on the mucosa, the dynamic stent was designed with a shape, more sophisticated than the shape of currently available endoprostheses. It is well acknowledged that the human trachea is not round in shape. The percentages of elliptical, C-, triangular and U-shaped tracheas and their dependance on sex and age have been well studied [19, 30, 31]. In addition, the shape of the trachea changes from the larynx towards the bifurcation. In order to reproduce as closely as possible the average shape of the trachea, we analysed cross-sections at three different levels. The mean of this analysis was taken for the casts of the stents. It is obvious that only rarely will an individual patient have a trachea of exactly this shape, but our stent was considered a clinically reasonable compromise. Measuring in a supine position (CT), we found the branching angle between the two main bronchi with 82±7° slightly bigger than the range of 70–80° that had been measured by others on plain chest X-rays of healthy subjects in the erect position [32, 33]. In expiration and in patients with mediastinal spread of cancer, higher angles of up to 100° have to be expected [33]. The flexibility of the silicone permits adaption of 15° without noticeable change in shape or cross-sectional area of the bronchial arms.

Compared to the tracheal section, the expansile forces of the bronchial limbs are limited as they are not reinforced by steel struts. Theoretically tumour compression could result in a collapse of these parts of the stent. However, adding metal rings would have complicated the insertion of the stent. As the stability of the silicone is comparable to the material used in the well-established Dumon bronchial stents [6, 14], we consider them safe enough.

Migration does not occur with the Montgomery T-tubes [34] or T-Y-tubes [1]. These prostheses are safe devices, but they lower the patient's quality of life due to the necessary tracheostomy and impaired speech. We addressed the problem of potential migration by designing a Y-shaped tracheobronchial stent. The bronchial arms of the stent anchor it and make migration nearly impossible. Furthermore, the dynamic properties of the stent allow rapid adaptions to increases in pressure by changing its shape; thereby, preventing migration under cough. Should the dynamic stent be displaced, its design prevents obstruction, as the folded bronchial limbs still provide for a sufficient lumen (fig. 11).

In conclusion, we have used theoretical considerations to guide the development of a bifurcated dynamic airway stent. With an *ex-vivo* model we tested its biomechanical behaviour. Our stent was found suitable for clinical application as it fulfilled two important requirements: cough ability and stability against tumour compression. At the time of writing we have inserted 141

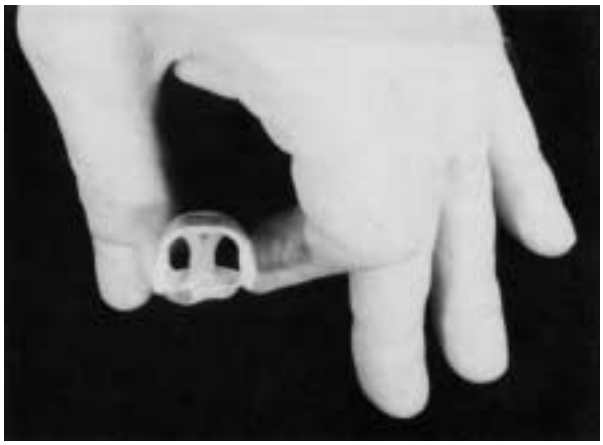

Fig. 11. – If the bronchial limbs are folded together, as during insertion or after cephalad migration, they still provide for a sufficient lumen.

dynamic stents into patients suffering from stenoses of the central airways and oesophagotracheal fistulae. A special forceps was developed that facilitates insertion of the bifurcated stent [35]. The expectations from the experimental work were fulfilled. The clinical results of the stent placements will be presented in a following paper. A multi-institutional study, testing efficacy and safety of the device is currently being performed.

Acknowledgements: The authors would like to thank F. Heimbrecht for writing the planimetry program and V. Freiburg for invaluable assistance in setting up the electronic equipment. They thank K Morgenroth (Bochum) for the excised human tracheae. The authors appreciate the assistance of A.B. Thompson, in the preparation of this manuscript.

References

1. Clarke DB. Palliative intubation of the trachea and main bronchi. *J Thorac Cardiovasc Surg* 1980; 80: 736–741.
2. Westaby S, Jackson JW, Pearson FG. A bifurcated silicone rubber stent for relief of tracheobronchial obstruction. *J Thorac Cardiovasc Surg* 1982; 83: 414–417.
3. Orlowski TM. Palliative intubation of the tracheobronchial tree. *J Thorac Cardiovasc Surg* 1987; 94: 343–348.
4. Wallace MJ, Charnsangavej C, Ogawa K, *et al*. Tracheobronchial tree: expandable metallic stents used in experimental and clinical applications. *Radiology* 1986; 158: 309–312.
5. Simonds AK, Irving JD, Clarke SW, Dick R. Use of expandable metal stents in the treatment of bronchial obstruction. *Thorax* 1989; 44: 680–681.
6. Dumon JF. A dedicated tracheobronchial stent. *Chest* 1990; 97(2): 328–332.
7. Varela A, Maynar M, Irving D, *et al*. Use of Gianturco self-expandable stents in the tracheobronchial tree. *Ann Thorac Surg* 1990; 49: 806–809.
8. Tsang V, Williams AM, Goldstraw P. Sequential silastic and expandable metal stenting for tracheobronchial strictures. *Ann Thorac Surg* 1992; 53: 856–860.
9. Mohnke M, Freitag L, Greschuchna D. Endobronchiale Prothesen - ein Erfahrungsbericht. *Pneumologie* 1991; 46: 148–152.
10. Agnew JE, Little F, Pavia D, Clarke SW. Mucus clearance from the airways in chronic bronchitic-smokers and ex-smokers. *Bull Eur Physiopathol Respir* 1982; 18: 473–484.
11. Ross BB, Gramiak R, Rahn H. Physical dynamics of the cough mechanism. *J Appl Physiol* 1955; 8: 264–268.
12. Royal JE. Tracheobronchial collapse during cough. *Radiology* 1965; 85: 87–92.
13. Morinari H, Sekine K, Yoshioka I, Tanaka M. Studies on dynamics of airway during cough. *Jap J Thorac Dis* 1982; 20: 547–552.
14. Colt HG, Dumon JF. Airway obstruction in cancer: the pros and cons of stents. *J Respir Dis* 1991; 12(8): 741–749.
15. Hankins WB. An endobronchial metallic prosthesis in the treatment of stenosis of the trachea. *Ann Otol Rhinol Laryngol* 1952; 61: 663–675.
16. Dobrin P, Canfield T. Cuffed endotracheal tubes: mucosal pressures and tracheal wall blood flow. *Am J Surg* 1977; 133: 562–565.
17. Nordin U. The trachea and cuff-induced tracheal injury. *Acta Otolaryngol (Stockholm)* 1977; 345s: 7–56.
18. Griscom NT. Cross-sectional shape of the child's trachea by computed tomography. *AJR* 1983; 140: 1103–1106.
19. Mackenzie CF, McAslan TC, Shin B, Schellinger D, Helrich M. The shape of the adult human trachea. *Anesthesiology* 1978; 49: 48–50.
20. Freitag L, Schroer M, Bremme J. High frequency oscillators with adjustable waveform: practical aspects. *Br J Anaesth* 1989; 63: 38–43.
21. Satoh S, Mori M, Inowe Y. Expandable metallic stents applied to benign bronchostenosis. *Chest* 1993; 103: 1302–1303.
22. Kim CS, Greene AG, Sankaran S, Sackner MA. Mucus transport in the airways by two-phase gas-liquid flow mechanism: continuous flow model. *J Appl Physiol* 1986; 60(3): 908–917.
23. Kim CS, Rodriguez CR, Eldridge MA, Sackner MA. Criteria for mucus transport in the airways by two-phase gas-liquid flow mechanism. *J Appl Physiol* 1986; 60(3): 901–907.
24. Soland V, Brock G, King M. Effect of airway wall flexibility on clearance by simulated cough. *J Appl Physiol* 1987; 63(2): 707–712.
25. Fallone BG, Wallace S, Gianturco C. Elastic characteristics of the self-expanding metallic stents. *Invest Radiol* 1988; 23: 370–376.
26. Shapiro AH. Steady flow in collapsible tubes. *J Biomech Eng* 1977; 99(3): 126–147.
27. Lambert RK. Bronchial mechanical properties and maximal expiratory flows. *J Appl Physiol* 1987; 62(6): 2426–2435.
28. Rains JK, Bert JL, Roberts CR, Paré PD. Mechanical properties of human tracheal cartilage. *J Appl Physiol* 1992; 72(1): 219–225.
29. Begis D, Delpuech C, Le Taallec P, Loth L, Thiriet M, Vidrascu M. A finite-element model of tracheal collapse. *J Appl Physiol* 1988; 64(4): 1359–1368.
30. Hartung W, Düweling A. Histomechanische Messungen an menschlichen Leichentracheen. *Med Thorac* 1964; 21: 257–274.
31. Mehta S, Myat HM. The cross-sectional shape and circumference of the human trachea. *Ann R Coll Surg (Engl)* 1984; 66(5): 356–358.
32. Birzle H. Das "Bifurkations-Veratmungstomogramm". *Fortschr Röntgenstr* 1959; 91: 483–487.
33. Brückner H. Die Auswirkung des Bronchial-Karzinoms auf die Atembeweglichkeit des Tracheobronchialbaumes, des Zwerchfells und des Brustkorbes. *Fortschr Röntgenstr* 1954; 80: 439–453.
34. Montgomery WW. T-tube tracheal stent. *Arch Otolaryngol* 1965; 82: 320–321.
35. Freitag L, Tekolf E, Greschuchna D. Development of a new insertion technique and a new device for the placement of bifurcated airway stents. *Surg Endoscopy* (in press).